

General Disclaimer

One or more of the Following Statements may affect this Document

- This document has been reproduced from the best copy furnished by the organizational source. It is being released in the interest of making available as much information as possible.
- This document may contain data, which exceeds the sheet parameters. It was furnished in this condition by the organizational source and is the best copy available.
- This document may contain tone-on-tone or color graphs, charts and/or pictures, which have been reproduced in black and white.
- This document is paginated as submitted by the original source.
- Portions of this document are not fully legible due to the historical nature of some of the material. However, it is the best reproduction available from the original submission.

NASA Technical Memorandum 86907

**(NASA-TM-86907) CHARACTERIZATION OF MMIC
DEVICES FOR ACTIVE ARRAY ANTENNAS (NASA)
17 p HC A02/MP A01 CSCL 09F**

N85-15779

**Unclas
G3/17 13103**

Characterization of MMIC Devices for Active Array Antennas

**Jerry Smetana
Lewis Research Center
Cleveland, Ohio**

and

**Everett Farr and Raj Mittra
University of Illinois
Urbana, Illinois**

**Prepared for the
1984 Antenna Applications Symposium
cosponsored by the University of Illinois and
the Rome Air Development Center (Bedford, MA)
Monticello, Illinois, September 19-21, 1984**

NASA



CHARACTERIZATION OF MMIC DEVICES FOR ACTIVE ARRAY ANTENNAS

Jerry Smetana
National Aeronautics and Space Administration
Lewis Research Center
Cleveland, Ohio 44135

and

Everett Farr and Raj Mittra
University of Illinois
Department of Electrical and Computer Engineering
Urbana, Illinois 61801

SUMMARY

It has become evident from NASA's active array technology development activities that more attention to the characterization of MMIC devices is needed. Having been fabricated using lithographic techniques, the MMIC has some inherently reproducible RF characteristics. NASA is currently sponsoring studies by the University of Illinois to investigate certain aspects of MMIC interconnectivity. These investigations are expected to contribute to a data base that will lead to providing for reproducible test results by the user as well as the manufacturer.

Some considerations are proposed that lead to preserving the inherently reproducible characteristics of the MMIC. It is highlighted that at radio frequencies (RF) greater than 20 GHz, the transition from the MMIC device to other transmission media must be an accurate RF match. It is proposed that the RF match is sufficiently critical to include the transition as part of the delivered MMIC package.

The model for analyzing several transitions will be presented. This model consists of a succession of abrupt discontinuities in printed circuit transmission lines. The analysis of these discontinuities is achieved with the Spectral Galerkin technique, to generate the modes and mode matching, to establish the generalized S-parameters of the individual discontinuities. Preliminary results achieved with this method are presented.

This paper concludes that special efforts should be coordinated by the active array antenna industry toward standardization of MMIC packaging and characterization.

INTRODUCTION

NASA is currently supporting technological development of fixed and scanning spot beam antenna systems at 20 and 30 GHz using monolithic microwave integrated circuit (MMIC) devices for active apertures. The approach is to develop the technology for the 20 GHz transmit antenna, then develop the 30 GHz receive antenna technology, finally combining the two technologies in to a 30/20 GHz system.

Figure 1 shows two typical configurations of (1) Multiple Fixed Spot Beam Antenna; and (2) Multiple Scanning Spot Beam Antenna Systems. The advantages of using MMIC modules in spacecraft antenna systems were discussed at the 1982 Antenna Applications Symposium (ref. 1). In summary, the advantages are:

- (1) Solid state power amplifiers (with distributed amplification)
- (2) Reliability through graceful degradation
- (3) Electronic beam steering
- (4) Phase and amplitude weightings for optimum performance
- (5) Dynamic reflector illumination control (as a function of scan angle)
- (6) FET switching (faster and more power conservative than PIN diode or ferrite switches)
- (7) Potential for lower weight and cost

In order to provide sufficiently high power (for operation in geostationary orbit) and effective illumination control, arrays with a large number of radiating elements (100 to 1000) may be required. In such large arrays where dynamic phase and amplitude controls will be implemented, it is important to accurately characterize the MMIC device. It is also important that after they are characterized (on a network analyzer, for example), their performance is the same as for the array antenna.

Another factor of great importance, when active high gain circuits are used in MMIC devices, is the stability of the packaged configuration. At frequencies greater than 20 GHz, the RF matching of the MMIC chip to a test station, as well as to the array antenna, is critical. Furthermore, when an array antenna is large, the multitude of long bias and control lines may be vulnerable to dispersion, crosstalk, or distortion from reflected pulses.

MMIC INTERCONNECTIVITY

Figure 2 illustrates the functional components of an MMIC and summarizes its interconnectivity. Three aspects of the interconnectivity are considered: the RF connection, the long DC or logic lines, and the heat transfer. This paper will focus on the importance of the RF connection. NASA is currently sponsoring studies on MMIC transitions under Grant NAG3-420 with the University of Illinois. Some results on the analysis of these transitions will be presented in the second half of this paper.

The MMIC having been fabricated with lithographic techniques can be expected to have some inherently reproducible RF characteristics. It is of great interest to preserve this reproducibility. In order to achieve this, one needs to provide a good transition or matching network at the RF input and output. In addition, some consideration must be given to the environment around the chip. For example, when MMIC chips have different sizes, the shielding around them can produce a variety of mismatched conditions. This paper will discuss some considerations in the design of transitions and the packaging of MMIC chips in terms of their impact on the characterization of MMIC devices.

CHARACTERIZATION OF MMIC DEVICES

At frequencies greater than 20 GHz, the required matching is so critical that, it is proposed, all of the matching should be included as part of the

MMIC packaging. It follows first of all that, since the MMIC device has a printed circuit type of RF input and output, it should be mounted on a printed circuit substrate. To preserve the reproducible RF characteristics of the MMIC, a pair of matching transitions from the chip to the substrate is needed. While figure 3 suggests a microstrip transmission line, the stripline or coplanar waveguide, for example, is also available.

One of the areas of MMIC packaging that will create a mismatch is the step change in the thickness of the chip and the substrate. The chip is typically 0.1 to 0.125 mm, while the substrate may be 0.5 to 1.5 mm thick. The two factors that determine the thickness of the substrate are heat dissipation and structural integrity. Both factors tend to increase the thickness. The presence of via-hole grounding tends to make the chip thinner. Figure 3 suggests a tapered ground plane as one solution to eliminating the step change. Another solution is to use the coplanar waveguide, which does not require a ground plane. Both solutions, however, present some difficulties, and more studies on trade-offs are needed to develop the best transition.

Another area that must be considered in the chip-to-substrate transition is the step change in the dielectric constant. A GaAs MMIC may have a relative dielectric constant greater than 12.3, while a variety of substrates available may have relative dielectric constants from 2.2 to 11.7. The material selected will most likely have the higher dielectric constant, unless there are thermal considerations. High-powered MMIC devices may require substrates with high thermal conductivities (e.g., such as boron nitride or beryllium oxide). The second half of this paper will present a more detailed analysis of step discontinuities.

Another consideration in the design of the module is that large gaps and long inductive leads must be avoided. In most cases, the MMIC device will be characterized on a network analyzer, which has waveguide or coaxial connectors. In addition, for many applications (e.g., such as an active array of horns), the MMIC device may have to be mounted in a waveguide or coaxial module. It then becomes necessary to include a second pair of transitions to match the substrate to the waveguide or coaxial line. Figure 3 shows a typical solution using the Van Heuven (ref. 2) microstrip-to-waveguide transition. Other waveguide transitions are being used, such as the ridged waveguide and the stripline. Figure 4 shows the three typical transitions mentioned above.

Figure 3 shows pads for connecting DC bias and logic lines. These are proposed for inclusion as part of the delivered package. Clearly, the MMIC device will be mounted in three or four test jigs or modules between fabrication and its final application. A place where bias and logic lines can be disconnected and reconnected is needed.

Not shown in figure 3, but an important consideration and inclusion, is the hermetic seal. A cover over the MMIC device of dielectric material (probably the same as the substrate) is needed to protect the chip from a humid or contaminated atmosphere. The cover must provide good isolation between the RF input and output lines.

In summary, the proposed MMIC package should include:

- (1) Printed circuit substrate
- (2) Transition from chip to substrate

- (3) Transition from substrate to waveguide (or coaxial line)
- (4) Tapered ground plane
- (5) Bias and logic line connection pads
- (6) Hermetic seal

To be avoided or minimized are:

- (1) Step discontinuities
- (2) Large gaps
- (3) Long inductive leads.

It is important that there be an understanding between the MMIC manufacturer and the user about all the conditions of the MMIC testing, in order to avoid disagreement between the results. In addition, it is important that in its final mode of operation (e.g., an array antenna), the MMIC has the same characteristics as it did in testing.

Figure 5 shows that, having fabricated the MMIC package of figure 3, it can be mounted in an easily fabricated housing. This housing can serve as a test jig as well as a module in an array antenna or any other waveguide circuit. When the MMIC package is mounted in the center of the waveguide, the waveguide is in the cut-off mode and the propagation is confined to the microstrip mode. The MMIC, therefore, can be easily installed into an identical environment at several test stations as well as its final operating location.

The University of Illinois and some in-house efforts at the NASA Lewis Research Center are expected to develop a data base on transitions and MMIC packaging. This data base can then be used by the MMIC industry, with some inputs of their own, to develop reproducible techniques for the characterization of MMIC devices.

The following sections describe a model for analyzing several transitions.

INTRODUCTION TO THE ANALYSIS

In order to determine which of the various transitions shown in figure 4 are most likely to fulfill the requirements outlined earlier in this paper, one would like to have the ability to analyze these configurations for insertion and return loss. If the S-parameters of these configurations can be determined, it should then be possible to design a configuration which has a relatively low insertion loss. The remainder of this paper will be devoted to developing the analytical tools one needs in order to characterize these transitions.

One problem that occurs with great frequency in the analysis of these transitions is an abrupt change in cross section of the printed circuit. An example of this is shown in figure 6. In this figure, a fin-line is tapered in steps to become a transition to rectangular waveguide. Thus, one may think of this transition as a succession of abrupt discontinuities in the printed circuit. If one can determine the S-parameters of each of these abrupt discontinuities, then it should be possible to cascade them together in a manner which will yield a low loss transition.

Abrupt printed circuit discontinuities may take a number of forms. The theory which is developed is general for many different types of discontinuities, as will be discussed later. For the present, however, it is necessary to begin by studying the most simple example of this discontinuity one can find. This turns out to be an abrupt change in the strip width of a shielded microstrip. A cross section of uniform shielded microstrip is shown in figure 7, and a discontinuity in the strip width is shown in figure 8. By studying this structure, it is hoped that the tools necessary to study a more realistic transition, such as the fin-line stepped taper shown previously in figure 1, will be developed.

The method to be used in the analysis of abrupt discontinuities involves mode matching in the plane of the discontinuity. In order to achieve this, one begins by generating the dominant and first few higher-order modes in each of the two microstrip lines. Next, one matches the tangential electric and magnetic field components in the plane of the discontinuity. Finally, one calculates the mode coefficients, which yield S-parameters and equivalent circuits of the discontinuity.

The study begins now with the analysis of the uniform microstrip.

ANALYSIS OF A UNIFORM MICROSTRIP

The first step in the analysis of a uniform microstrip involves finding a Green's function which relates currents on the strip to the electric fields at all other points in the cross section of the line. This is accomplished by solving a two-dimensional Helmholtz equation in regions I and II.

$$\left(\nabla^2 + k_1^2\right) \begin{Bmatrix} \phi_1 \\ \psi_1 \end{Bmatrix} = 0 \quad (1a)$$

$$k_1 = \omega \sqrt{\mu_0 \epsilon_1} \quad (1b)$$

$$\epsilon_1 = \begin{cases} \epsilon_1 & x > 0 \\ \epsilon_1 \epsilon_r & x < 0 \end{cases} \quad (1c)$$

In the above equations, 1 denotes the region, and ϕ_1 and ψ_1 are the electric and magnetic scalar potentials in each region.

It is convenient to solve the above equation in the spectral domain, so one takes the Fourier transform of all potentials and fields as

$$\tilde{\phi}(n, y) = \int_{-\infty}^{\infty} \phi(x, y) e^{j\alpha_n x} dx \quad (2a)$$

$$\phi(x, y) = \frac{1}{2b} \sum_{-\infty}^{\infty} \tilde{\phi}(n, y) e^{-j\alpha_n x} \quad (2b)$$

$$\alpha_n = \frac{n\pi}{b} \quad (2c)$$

By matching boundary conditions on the shield walls and on the center conductor, one obtains an equation of the form

$$\begin{bmatrix} \tilde{Z}_{zz}(\alpha_n, \beta) & \tilde{Z}_{zx}(\alpha_n, \beta) \\ \tilde{Z}_{xz}(\alpha_n, \beta) & \tilde{Z}_{xx}(\alpha_n, \beta) \end{bmatrix} \begin{bmatrix} \tilde{J}_z(\alpha_n) \\ \tilde{J}_x(\alpha_n) \end{bmatrix} = \begin{bmatrix} \tilde{E}_z(\alpha_n, \beta) \\ \tilde{E}_x(\alpha_n, \beta) \end{bmatrix} \quad (3)$$

This equation relates the current in the plane $y = 0$ to the electric fields in this plane. The dyadic Green's function, $\tilde{Z}_{ij}(\alpha_n, \beta)$, consists of relatively simple expressions in terms of hyperbolic sines and cosines.

Before proceeding to the solution of this equation for β , one should first look at the methods for generalizing the above Green's function. The above method is satisfactory for configurations with one dielectric layer and one strip. But a method developed by T. Itoh (ref. 3) gives a technique for generating a Green's function for structures with an arbitrary number of dielectric layers and conducting strips. His technique is called the Spectral Impedance Approach. While a detailed explanation of the technique is beyond the scope of this paper, it may be stated that the technique involves the separation of the fields in each dielectric region into TE_y and TM_y components in the spectral domain, and the subsequent formulation of analogous transmission lines in the \hat{y} direction for the decoupled TE and TM fields. This generalization extends the applicability of the techniques presented in this paper to a large class of printed circuits.

Next, one must find the solution to the integral equation shown in equation (3). The solution is effected by the spectral Galerkin technique (ref. 4), in which a moment method solution is brought about in the spectral domain. Hence, the current on the strip is expanded in terms of basis functions, which are nonzero only on the strip, as

$$J_z(x) = \sum_{l=1}^N c_l \frac{\cos[(l-1)\pi(x/s) - 1]}{\sqrt{1 - (x/s)^2}} \quad (4a)$$

$$J_x(x) = \sum_{l=1}^N d_l \frac{\sin(l\pi(x/s) - 1)}{\sqrt{1 - (x/s)^2}} \quad (4b)$$

One then takes the Fourier transform of these currents and substitutes the result into equation (3). Next, the inner product of the resulting equation is taken with the individual basis functions, and Parseval's theorem is used to eliminate the right-hand side. The resulting matrix equation may be solved by setting the determinant equal to zero and solving for β with Newton's method.

The accuracy of this method is determined by the number of basis functions and the number of spectral terms one can calculate within a reasonable amount of computer time. For the dominant mode and lower-order evanescent modes, a small number of basis functions and spectral terms is probably satisfactory.

For evanescent modes of larger order, it is likely that more basis functions and spectral terms are required to achieve reasonable accuracy.

Sample calculations were carried out in order to calculate the dominant and first two evanescent modes of microstrip. These results are shown in figure 9. One would like to compare these modes to other results, but little data are available on microstrip modes. The microstrip mode calculations that are available deal with propagating modes, but do not present data on evanescent modes (refs. 5 and 6). There does exist, however, one paper which presents calculations of fin-line for both propagating and evanescent modes (ref. 7). In order to adapt our analysis to fin-line, we need only to change the dyadic Green's function, \bar{Z}_{ij} . This was done, and a dispersion curve was calculated (fig. 10). Clearly, satisfactory agreement with the results in reference 7 has been achieved. Since the microstrip calculation is quite similar to the fin-line calculation, it is believed that the microstrip mode calculations should also be reasonable.

Once the modes have been found and verified, the next step is to calculate the characteristic impedance of the uniform line. This is done for two reasons. First, it gives added confirmation that the dominant mode calculation is accurate. Second, it gives a first-order approximation to the input impedance at a discontinuity. This result is useful as a comparison for results obtained with the mode matching technique. Since the characteristic impedance is defined only for TEM lines, one must be careful to choose a definition of characteristic impedance which is useful experimentally. The definition most commonly chosen is the power-current definition.

$$Z_0 = \frac{2P}{II^*} \quad (5a)$$

$$P = 1/2 \operatorname{Re} \iint \bar{E} \times \bar{H}^* dx dy \quad (5b)$$

$$I = \int_{-s}^s J_z(x) dx \quad (5c)$$

An alternative definition is the voltage-current definition

$$Z_0 = \frac{V}{I} \quad (6a)$$

$$V = - \int_{-d}^0 E_y(y) dy \Big|_{x=0} \quad (6b)$$

Calculations were performed with both of these definitions, and are plotted in figure 11. They correspond very well with data already published in reference 6.

ANALYSIS OF DISCONTINUITIES WITH MODE MATCHING

Among the techniques for studying waveguide discontinuities, mode matching seems one of the most promising (ref. 8, part 4). This technique is suitable for calculating the characteristics of abrupt discontinuities, such as those in

figures 6 and 8. In addition, this method is easily adaptable to a cascade of abrupt discontinuities by using generalized S-parameters. Finally, it may be possible to model a smooth taper as a cascade of step discontinuities. Hence, the mode matching technique is capable of solving a wide variety of problems.

The mode matching technique begins by using the modes of the uniform microstrip calculated in the previous section. This involves finding the transverse fields for each mode and in each of the two waveguides.

$$\tilde{e}_{1a}(n,y) = \tilde{e}_{x1a}(n,y)\hat{x} + \tilde{e}_{y1a}(n,y)\hat{y} \quad (7a)$$

$$\tilde{h}_{1a}(n,y) = \tilde{h}_{x1a}(n,y)\hat{x} + \tilde{h}_{y1a}(n,y)\hat{y} \quad (7b)$$

where i denotes the mode number, and a denotes that we are referring to the input waveguide. Similar expressions hold for the output waveguide. At the point of the discontinuity, these transverse fields must be continuous. Enforcing this boundary condition, one obtains

$$(1 + \rho)a_1\tilde{e}_{a1} + \sum_{i=2}^{\infty} a_i\tilde{e}_{ai} = \sum_{j=1}^{\infty} b_j\tilde{e}_{bj} \quad (8a)$$

$$(1 - \rho)a_1\tilde{h}_{a1} - \sum_{i=2}^{\infty} a_i\tilde{h}_{ai} = \sum_{j=1}^{\infty} b_j\tilde{e}_{bj} \quad (8b)$$

where ρ is the reflection coefficient of the dominant mode, and a_i and b_j are the amplitudes of the modes in waveguides a and b , respectively. At this point, one takes appropriate inner products of equation (8) and forms a matrix equation for ρ and for the mode coefficients a_i and b_j . Once these have been found, equivalent circuit parameters, Z_n and Y_n , are calculated as shown in figure 12. The circuit has now been characterized completely.

When using the above method, it is necessary to find an alternate method of calculating the equivalent circuit parameters. This gives approximate values for Z_n and Y_n , against which one can compare the results derived from the mode matching technique. The only alternate method in the literature which treats this problem uses a static technique, which is valid only for lower frequencies. An example of this technique is shown in reference 9. Therefore, a lower frequency case was chosen for the initial study, in order to be able to compare the results with other sources. If the validity of the mode matching technique can be demonstrated at lower frequencies, one may assume the technique is valid also at higher frequencies.

By calculating a low frequency case, one is able to compare the results for Z_n and Y_n to calculations made with other methods. In this case, Z_n is approximated by the normalized characteristic impedance of waveguide 2, relative to waveguide 1. The power-current definition of characteristic impedance is used (eq. (5)). Furthermore, one can get an approximation to Y_n by referring to the junction capacitances calculated in figure 12.

A sample case of a microstrip discontinuity calculation is shown in figure 12. The equivalent circuit parameters, Z_n and Y_n , are plotted as a

function of the number of waveguide modes used. The convergence of the normalized input impedance, Z_n , to its correct value has been demonstrated. The input admittance Y_n , however, seems to be dependent upon the number of modes used in each guide. It is necessary to get Y_n to converge in order to obtain the junction capacitance. It is likely that improved convergence of Y_n can be obtained by improving the efficiency of the inner product calculation, thus allowing the use of more modes in the mode matching technique.

There are many areas in this technique where additional study is needed. First, the sensitivity of the final answer to the number of spectral terms, the number of basis functions, and the number of modes used must be checked. Next, it is necessary to eliminate the dependency on the number of spectral terms used, by implementing an asymptotic form for the calculation of spectral terms of very large order. This change should reduce the computation time significantly. Finally, this technique should be applied to a variety of different structures such as those shown in figures 4 and 6, and other structures useful in transitions between printed circuits and rectangular waveguides.

CONCLUDING REMARKS

Having been fabricated with lithographic techniques, the MMIC has inherently reproducible RF characteristics. In order to preserve the reproducibility of the MMIC and to be able to characterize MMIC devices with reproducible results, the following considerations have been proposed: (1) mount the device on a printed circuit substrate; (2) provide an accurate transition from chip to substrate; (3) provide an accurate transition from substrate to waveguide; (4) eliminate discontinuities; (5) provide DC and logic connection pads; (6) provide a hermetic seal; and (7) include these in the delivered package. The importance of reproducible characterization by manufacturer and user was discussed.

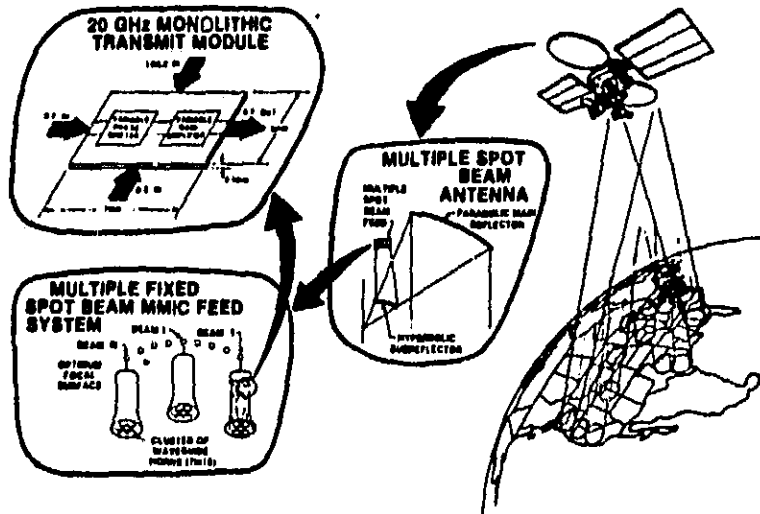
A model for analyzing several types of transitions was described. The model involved the breakdown of transitions into a cascade of abrupt printed circuit discontinuities, whose S-parameters were determined with mode matching techniques. The initial results presented in this report demonstrate the method to be a promising one.

REFERENCES

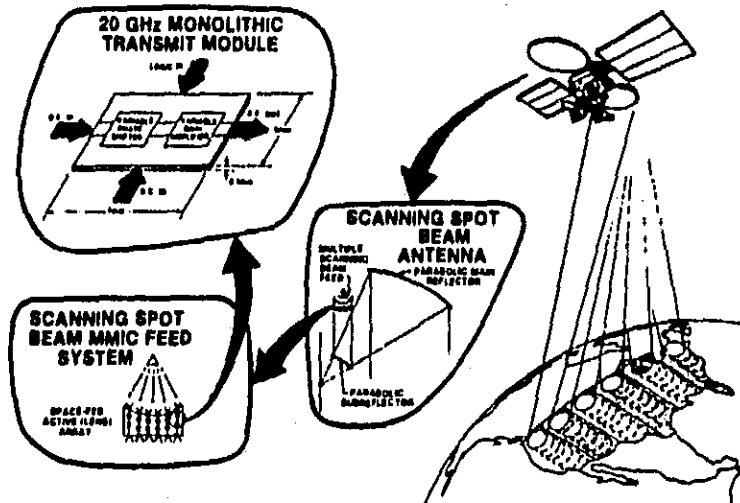
1. Smetana, J. (1982) Application of MMIC modules in future multiple beam satellite antenna systems, NASA Technical Memorandum 83344.
2. Van Heuven, J.H.C. (1976) A new integrated waveguide-microstrip transition, IEEE Trans. Microwave Theory Tech., MTT-24:144-147.
3. Itoh, T. (1980) Spectral domain immittance approach for dispersion characteristics of generalized printed transmission lines, IEEE Trans. Microwave Theory Tech., MTT-28:733-736.
4. Schmidt, L.P. and Itoh, T. (1980) Spectral domain analysis of dominant and higher order modes in fin-lines, IEEE Trans. Microwave Theory Tech., MTT-28:981-985.

5. Mirshekar-Syahkal, D. and Davies, J.B. (1979) Accurate solution of microstrip and coplanar structures for dispersion and for dielectric and conductor losses, IEEE Trans. Microwave Theory Tech., MTT-27:694-699.
6. El-Sherbiny, A.M.A. (1981) Accurate analysis of shielded microstrip lines and bilateral fin-lines, IEEE Trans. Microwave Theory Tech., MTT-29:669-675.
7. Helard, M. et al. (1983) Exact calculations of scattering parameters of a step slot width discontinuity in a unilateral fin-line, Electron. Lett., 19:537-539.
8. El-Hennawy, H. and Schunemann, K. (1982) Impedance transformation in fin-lines, IEEE Proc., 129:342-350.
9. Horton, R. (1973) Equivalent representation of an abrupt impedance step in microstrip line, IEEE Trans. Microwave Theory Tech., MTT-21:562-564.

ORIGINAL PAGE IS
OF POOR QUALITY



(a) Multiple fixed spot beam antenna.



(b) Multiple scanning spot beam antenna.

CD-84-15911

Figure 1. - 30/20 GHz satellite communications antenna systems.

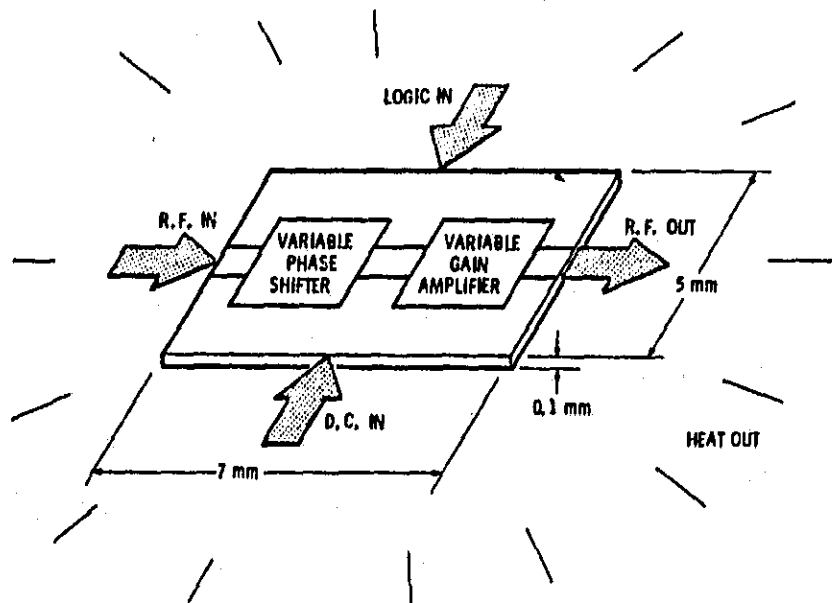


Figure 2. - MMIC Interconnectivity.

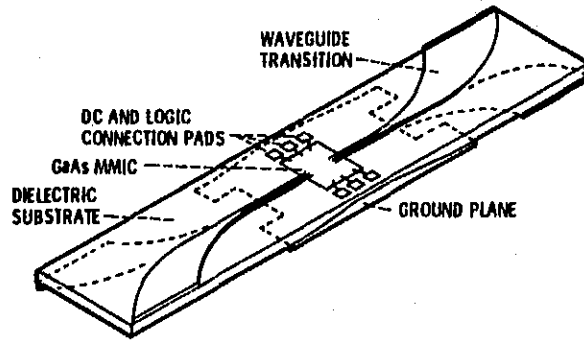
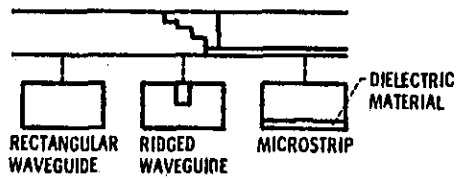
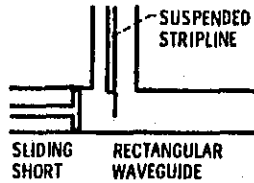


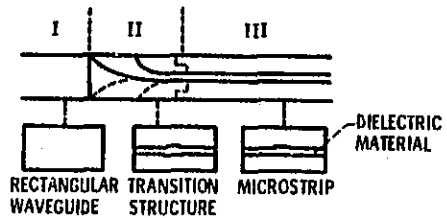
Figure 3 - packaging configuration.



(a) Stepped ridgeline transition.



(b) Stripline probe transition.



(c) Van Heuven transition.

Figure 4. - Typical substrate-to-waveguide transitions.

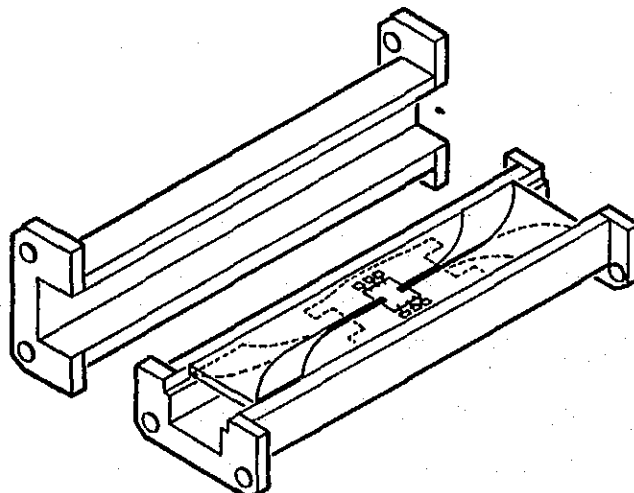


Figure 5. - Typical MMIC environment.

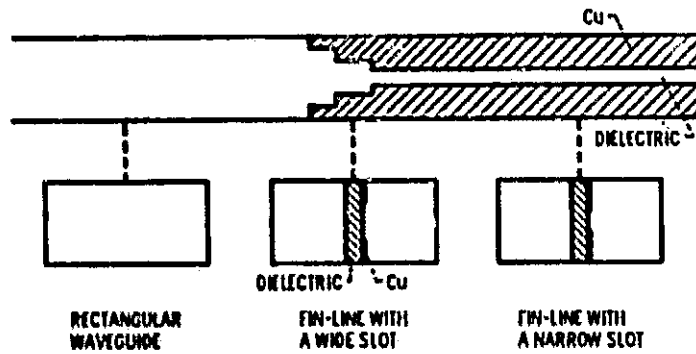


Figure 6. - Transition between fin-line and rectangular waveguide.

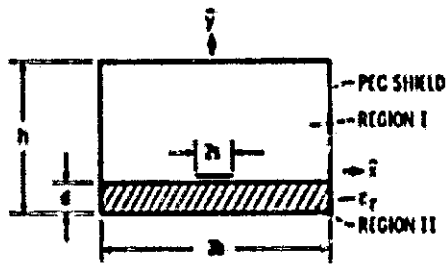


Figure 7. - Cross section of shielded microstrip.



Figure 8. - Top view of a discontinuity in the strip width on a microstrip.

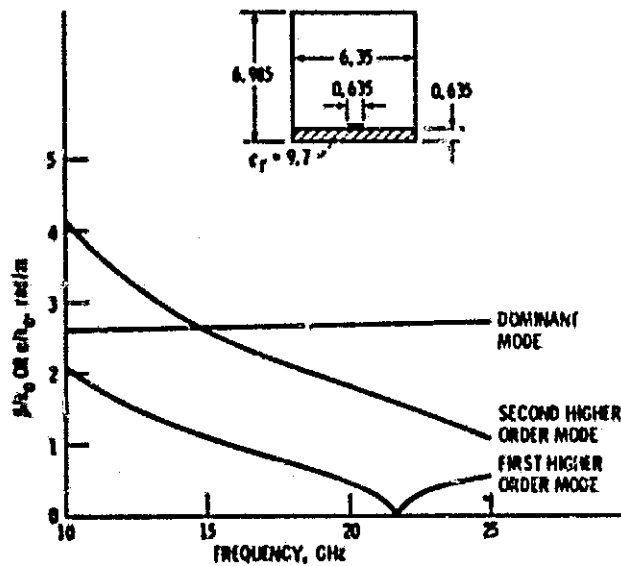


Figure 9. - The dispersion characteristics of the dominant and first two even higher-order modes of microstrip. Two basis functions and 201 spectral terms were used. (Dimensions in mm.)

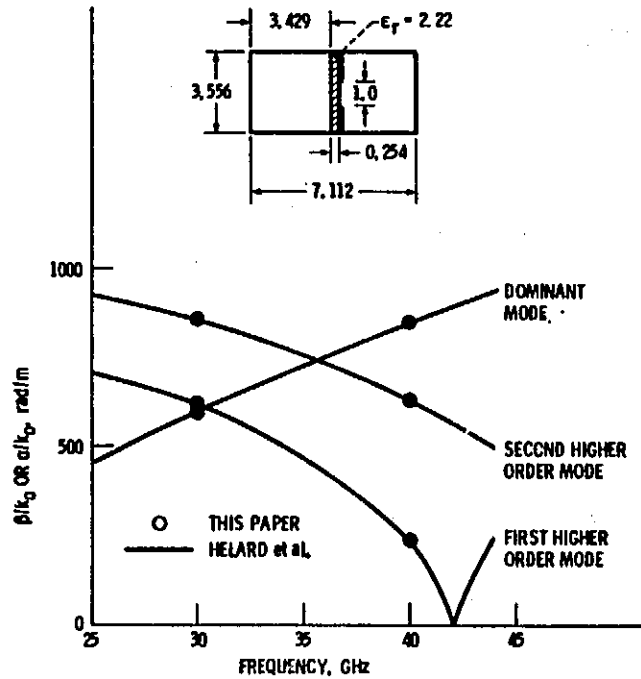


Figure 10. - Dispersion curve of fin-line. Calculated with one basis function and 101 spectral terms. (Dimensions in mm.)

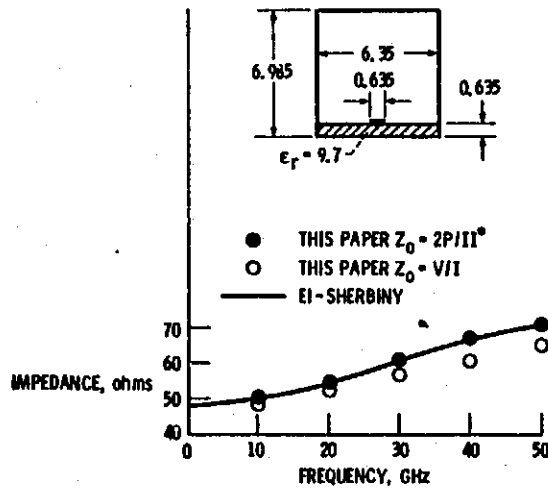


Figure 11. - Characteristic impedance of microstrip using two definitions. Calculated with one basis function and 101 spectral terms.

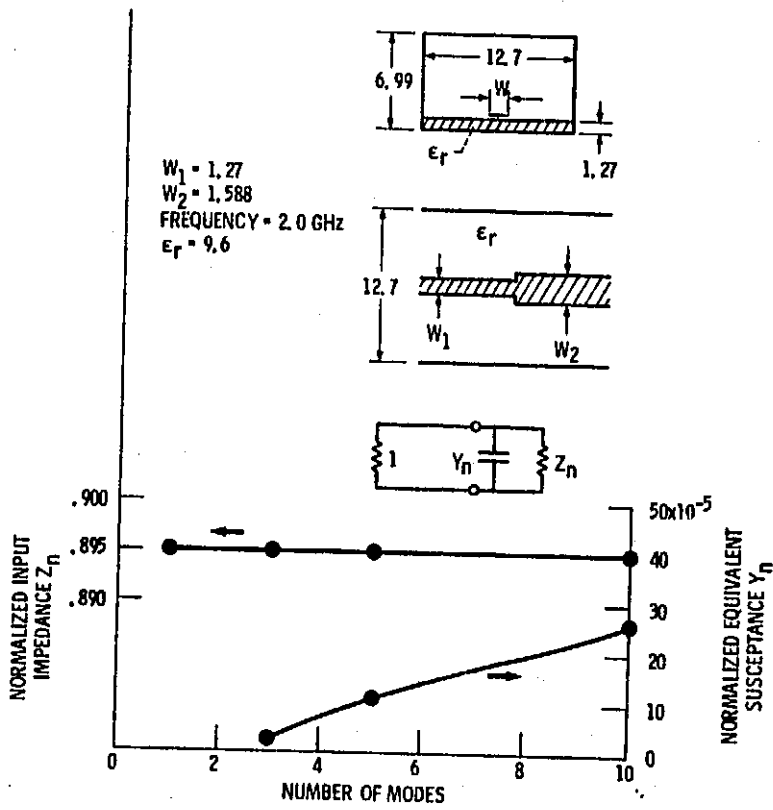


Figure 12 - Variation of normalized impedance and normalized susceptance with the number of waveguide modes. Calculated with one basis function and 101 spectral terms. It is expected that $Z_n = 0.895$ and $Y_n = 128 \times 10^{-5}$. (Dimensions in mm.)